

A posteriori error analysis of the virtual element method for second-order quasilinear elliptic PDEs

Scott Congreve and Alice Hodson*

Abstract

In this paper we develop a C^0 -conforming virtual element method (VEM) for a class of second-order quasilinear elliptic PDEs in two dimensions. We present a posteriori error analysis for this problem and derive a residual based error estimator. The estimator is fully computable and we prove upper and lower bounds of the error estimator which are explicit in the local mesh size. We use the estimator to drive an adaptive mesh refinement algorithm. A handful of numerical test problems are carried out to study the performance of the proposed error indicator.

Keywords. virtual element method; a posteriori error analysis; adaptivity; quasilinear elliptic PDEs; nonlinear; DUNE.

1 Introduction

In this paper we present a conforming virtual element method (VEM) of arbitrary order for the numerical solution of a quasilinear elliptic problem in two dimensions. We consider the *a posteriori* error analysis in the H^1 -seminorm of the virtual element method for the following boundary value problem:

$$\begin{aligned} -\nabla \cdot (\mu(\mathbf{x}, |\nabla u|) \nabla u) &= f \quad \text{in } \Omega, \\ u &= 0 \quad \text{on } \partial\Omega \end{aligned} \tag{1.1}$$

for a polygonal domain $\Omega \subset \mathbb{R}^2$ and $f \in L^2(\Omega)$. For ease of presentation, we only consider homogeneous Dirichlet boundary value problems. Furthermore, we assume that the nonlinearity μ satisfies the following set of standard assumptions see e.g. [37].

*Corresponding author (hodson@karlin.mff.cuni.cz).

Charles University, Faculty of Mathematics and Physics, Sokolovská 83, 186 75, Praha, Czech Republic

Assumption 1.1 (Nonlinearity assumptions). We assume that the nonlinearity μ satisfies the following conditions.

$$(a) \ \mu \in C^0(\overline{\Omega} \times [0, \infty))$$

(b) There exist positive constants m_μ, M_μ such that

$$m_\mu(t-s) \leq \mu(\mathbf{x}, t)t - \mu(\mathbf{x}, s)s \leq M_\mu(t-s), \quad t \geq s \geq 0, \text{ for all } \mathbf{x} \in \overline{\Omega}.$$

Importantly, if μ satisfies (b) in Assumption 1.1, then it can be shown that there exist constants C_1, C_2 with $C_1 \geq C_2 > 0$ such that for any $v, w \in \mathbb{R}^2$ and $\mathbf{x} \in \overline{\Omega}$,

$$|\mu(\mathbf{x}, |v|)v - \mu(\mathbf{x}, |w|)w| \leq C_1|v - w|, \quad (1.2)$$

and

$$C_2|v - w|^2 \leq (\mu(\mathbf{x}, |v|)v - \mu(\mathbf{x}, |w|)w) \cdot (v - w); \quad (1.3)$$

cf., [38, Lemma 2.1]. We note that the above assumptions are fulfilled by several physical models from continuum mechanics; e.g., the Carreau law

$$\mu(\mathbf{x}, t) = k_\infty + (k_0 - k_\infty)(1 + \lambda t^2)^{(\theta-2)/2},$$

with $k_0 > k_\infty > 0$ and $\theta \in (1, 2]$. Moreover, it is worth mentioning that studying problem (1.1) is an important stepping stone in deriving efficient and effective numerical methods for non-Newtonian flow problems, see e.g. [24] and the references therein.

Introduced in 2013 [12], the virtual element method is an extended and generalised version of the finite element and mimetic finite difference methods and was first introduced in the context of second-order elliptic problems. The method is highly advantageous for many reasons including the ease with which the method extends to general polygonal and polyhedral meshes. This is extremely beneficial especially when developing adaptive schemes, since hanging nodes are automatically permissible within the VEM framework. Furthermore, their versatility has been showcased by the wide range of problems they have been applied to over the past 10 years. These include, but are not limited to, the following: the development of higher order continuity spaces [9, 10], H^m -conforming VEM in any dimension [21], as well as the application to nonlinear problems such as the steady Navier-Stokes equation [13] where the discrete velocity field is shown to be pointwise divergence-free. We note that the first adaptive VEM schemes appeared in [14, 15, 19] and additional further developments of VEM and its applications can be found in the recent book [5].

A virtual element discretisation of a quasilinear diffusion problem in both two and three dimensions is considered in [18], while a two grid virtual element algorithm is developed in [22] and a priori estimates in the H^1 -norm are derived. Other polygonal methods which have been considered for the discretisation of problem (1.1) can be found in the

following works: the mimetic finite difference (MFD) method is analysed in [7] where only a lowest order approximation is considered and no a posteriori analysis is carried out, an HHO method for a general class of Leray-Lions elliptic equations (including the problem considered in this paper) is presented in [31] as well as a class of quasilinear elliptic problems of nonmonotone type are analysed in [35]. Similarly to the MFD case, only a priori estimates are shown.

In this paper we present a virtual element method for problem (1.1). We introduce a C^0 -conforming VEM based on those introduced in [2, 20] where we follow the projection approach detailed in [26, 27]. In this approach, the projection operators are defined without using the underlying variational problem, allowing us to apply the method directly to nonlinear problems including quasilinear problems such as (1.1). We note that the same projection method has also been applied to the nonlinear fourth-order Cahn-Hilliard equation in [25]; however, only a priori error analysis is carried out in this case. The aforementioned projection method involves defining a hierarchy of projections, starting with a constrained least squares (CLS) problem for the value projection. All projections are fully computable from the degrees of freedom (dofs) and are shown to be L^2 projections. In this work, we employ this hierarchical projection approach in our discrete construction. Consequently, we are able to discretise the nonlinearity μ directly using the gradient projection, which itself is an L^2 projection of the gradient [26]. This approach avoids complicated averaging techniques seen in e.g. [6] where special treatment of the nonlinearity is required and thus restricted their approach to a lowest order approximation.

Virtual element methods for quasilinear problems have been studied in [18]; however, in contrast to the results shown in [18], we present an a posteriori analysis which follows the ideas introduced in [19]. We carry out the analysis under the same regularity assumptions required in the linear setting [12] thus allowing very general polygonal meshes, which we exploit in our adaptive algorithm. To the best of our knowledge, this work is the first a posteriori error analysis for a virtual element discretisation of elliptic quasilinear problems on general polygonal meshes.

The structure of this paper is as follows. In section 2 we introduce the proposed virtual element method and setup the discrete projections, spaces, and forms. Furthermore, by employing results from the theory of monotone operators, we show that the discrete problem has a unique solution. We carry out the a posteriori error analysis in section 3, deriving a reliable and efficient residual based error estimator. We carry out a series of numerical experiments in section 4 and use the estimator to drive an adaptive algorithm. Finally, concluding remarks are given in section 5.

Throughout this paper we adopt the standard notation for Sobolev spaces $H^s(\mathcal{D})$ for nonnegative integers s , and domains \mathcal{D} , with the norm and seminorm denoted by $\|\cdot\|_{s,\mathcal{D}}$ and $|\cdot|_{s,\mathcal{D}}$, respectively. When $\mathcal{D} = \Omega$ we may omit the subscript.

We first write problem (1.1) in variational form: find $u \in H_0^1(\Omega)$ such that

$$a(u; u, v) = (f, v), \quad \forall v \in H_0^1(\Omega), \quad (1.4)$$

where the form a is given by $a(u; v, w) := (\mu(\mathbf{x}, |\nabla u|) \nabla v, \nabla w)$ and (\cdot, \cdot) denotes the standard L^2 inner product over Ω . We note that, assuming sufficient regularity for the right hand side f , problem (1.1) admits a unique solution, see e.g. [33].

2 The virtual element method

In this section, we discuss the numerical approximation of problem (1.1) by the virtual element method. Following the discretisation approach in [2, 20], we use the so called “VEM enhancement” technique (which has been extended to fourth-order problems in [26]) to discretise problem (1.4).

2.1 Mesh regularity and a polynomial approximation result

Let \mathcal{T}_h denote a tessellation of the computational domain $\Omega \subset \mathbb{R}^2$ into simple nonoverlapping polygons E such that $\overline{\Omega} = \bigcup_{E \in \mathcal{T}_h} E$. We denote by $h_E := \text{diam}(E)$ the diameter of $E \in \mathcal{T}_h$ and let $h = \max_{E \in \mathcal{T}_h} h_E$ denote the maximum diameter of all elements. We define the set of all edges in the mesh by \mathcal{E}_h , which we split into boundary edges \mathcal{E}_h^{bdy} and interior edges \mathcal{E}_h^{int} , such that $\mathcal{E}_h^{bdy} := \{e \in \mathcal{E}_h : e \subset \partial\Omega\}$ and $\mathcal{E}_h^{int} = \mathcal{E}_h \setminus \mathcal{E}_h^{bdy}$.

Let \mathbf{v} be a vector-valued function, which is smooth inside each element $E \in \mathcal{T}_h$. Given two adjacent elements $E^+, E^- \in \mathcal{T}_h$ sharing a common edge $e \in \mathcal{E}_h^{int}$, i.e., $e \subset \partial E^+ \cap \partial E^-$, we write \mathbf{v}^\pm to denote the trace of $\mathbf{v}|_{E^\pm}$ on the edge e taken from the interior of E^\pm , respectively. We then define the jump operator across the edge $e \in \mathcal{E}_h$ as follows: $\llbracket \mathbf{v} \rrbracket := \mathbf{v}^+ \cdot \mathbf{n}_e^+ + \mathbf{v}^- \cdot \mathbf{n}_e^-$ where \mathbf{n}_e^\pm denotes the unit outward normal on e from E^\pm , respectively. On a boundary edge, $e \in \mathcal{E}_h^{bdy}$, we let $\llbracket \mathbf{v} \rrbracket := \mathbf{v} \cdot \mathbf{n}_e$, where \mathbf{n}_e is the unit outward normal on $\partial\Omega$.

Assumption 2.1 (Mesh regularity assumptions). We assume there exists a constant $\rho > 0$ such that

- (a) each element of the mesh $E \in \mathcal{T}_h$ is star-shaped with respect to a ball of radius ρh_E , and
- (b) $h_e \geq \rho h_E$ for every element $E \in \mathcal{T}_h$ and every edge $e \subset \partial E$.

Note that these assumptions are standard in the virtual element setting as found in [12].

Remark 2.2. Importantly, we note that as a consequence of the above, each element $E \in \mathcal{T}_h$ admits a sub-triangulation; i.e., a partition of E into triangles. This can be

obtained by joining each vertex of E to a point \mathbf{x}_E in E such that E is star shaped with respect to \mathbf{x}_E .

For any $k \in \mathbb{N}$, we denote by $\mathbb{P}_k(D)$ the space of polynomials of degree at most k on $D \subset \mathbb{R}^d$, $d = 1, 2$. In practice, D is either an element $E \in \mathcal{T}_h$ or an edge $e \in \mathcal{E}_h$. For an element $E \in \mathcal{T}_h$, we denote by $\mathcal{P}_k^E : L^2(E) \rightarrow \mathbb{P}_k(E)$ the L^2 -orthogonal projection onto $\mathbb{P}_k(E)$. The following theorem is an important result for the theory in section 3, the proof of which can be obtained following the theory in either [17, 23].

Theorem 2.3 (Approximation using polynomials). *Under Assumption 2.1, for any $k \geq 0$ and for any $w \in H^m(E)$ with $1 \leq m \leq k + 1$, it holds that*

$$\|w - \mathcal{P}_k^E w\|_{0,E} + h_E |w - \mathcal{P}_k^E w|_{1,E} \leq C_3 h_E^m |w|_{m,E}$$

where the constant C_3 depends only on k and the mesh regularity.

Furthermore, we note that we can split the form $a(\cdot; \cdot, \cdot)$ and norm $|\cdot|_1$ as

$$\begin{aligned} a(u; v, w) &:= \sum_{E \in \mathcal{T}_h} a^E(u; v, w) = \sum_{E \in \mathcal{T}_h} (\mu(\mathbf{x}, |\nabla u|) \nabla v, \nabla w)_E, \quad \forall u, v, w \in H_0^1(\Omega), \\ |v|_1 &:= \left(\sum_{E \in \mathcal{T}_h} |v|_{1,E}^2 \right)^{1/2} \quad \forall v \in H_0^1(\Omega). \end{aligned}$$

2.2 The discrete spaces and projection operators

In this section, our aim is to build a discrete VEM space $V_{h,\ell} \subset H_0^1(\Omega)$ of polynomial order $\ell \geq 1$, our order of approximation, such that, for each $E \in \mathcal{T}_h$, $\mathbb{P}_\ell(E) \subset V_{h,\ell}|_E$. The other crucial aspect of the virtual element discretisation is the construction of suitable fully computable projection operators Π_0^E, Π_1^E .

To this end, we begin by building an enlarged VEM space $\tilde{V}_{h,\ell}^E$ and an appropriate set of extended *degrees of freedom* (dofs) for this space. We then introduce a reduced set of dofs for $V_{h,\ell}^E$ and use these dofs to construct *dof compatible* projection operators, which will be used to define the local VEM space as well as the discrete forms. Further details for topics in this section can be found in [26].

Definition 2.4. For an element $E \in \mathcal{T}_h$ we define the *enlarged VEM space* as

$$\tilde{V}_{h,\ell}^E := \{v_h \in H^1(E) : \Delta v_h \in \mathbb{P}_\ell(E) \text{ and } v_h|_e \in \mathbb{P}_\ell(e) \forall e \subset \partial E\},$$

which we characterise by the set of extended degrees of freedom $\tilde{\Lambda}^E$ described using the *dof tuple* notation introduced in [26]; i.e., $\tilde{\Lambda}^E$ is characterised by the dof tuple

$$(0, -1, \ell - 2, -1, \ell).$$

That is, the dofs $\tilde{\Lambda}^E$ characterising the enlarged VEM space for $v_h \in H^1(E)$ are:

- (D1) The value of v_h at each vertex of E .
- (D2) For $\ell > 1$, the moments of v_h up to order $\ell - 2$ on each edge $e \subset \partial E$

$$\frac{1}{|e|} \int_e v_h p \, ds \quad \forall p \in \mathbb{P}_{\ell-2}(e).$$

- (D3) For $\ell > 1$, the moments of v_h up to order ℓ inside E

$$\frac{1}{|E|} \int_E v_h p \, ds \quad \forall p \in \mathbb{P}_\ell(E).$$

A proof of the unisolvency of these degrees of freedom can be found in [20].

We can now define the local VEM space $V_{h,\ell}^E$, for an element $E \in \mathcal{T}_h$, as a subspace of the enlarged space $\tilde{V}_{h,\ell}^E$. In order to do so, we first introduce an interior value projection $\Pi_0^E : \tilde{V}_{h,\ell}^E \rightarrow \mathbb{P}_\ell(E)$ and an edge value projection $\Pi_0^e : \tilde{V}_{h,\ell}^E \rightarrow \mathbb{P}_\ell(e)$. These projections must be computable from the reduced set of degrees of freedom Λ^E , described by the dof tuple,

$$(0, -1, \ell - 2, -1, \ell - 2); \quad (2.1)$$

i.e., Λ^E consists of the original dofs introduced in e.g. [12] for second-order problems. We also require that these projections satisfy the following assumptions.

Assumption 2.5. For $v_h \in \tilde{V}_{h,\ell}^E$, we assume that the value and edge projection operators Π_0^E and Π_0^e are a linear combination of the degrees of freedom $\Lambda^E(v_h)$. Furthermore, we assume they satisfy the following properties.

- (a) The value projection $\Pi_0^E v_h \in \mathbb{P}_\ell(E)$ satisfies

$$\int_E \Pi_0^E v_h p \, dx = \int_E v_h p \, dx \quad \forall p \in \mathbb{P}_{\ell-2}(E)$$

and $\Pi_0^E q = q$ for all $q \in \mathbb{P}_\ell(E)$.

- (b) For each edge $e \subset \partial E$, the edge projection $\Pi_0^e \in \mathbb{P}_\ell(e)$ satisfies $\Pi_0^e v_h(e^\pm) = v_h(e^\pm)$, where e^\pm denotes the vertices of an edge e ,

$$\int_e \Pi_0^e v_h p \, ds = \int_e v_h p \, ds \quad \forall p \in \mathbb{P}_{\ell-2}(e),$$

and $\Pi_0^e q = q|_e$ for all $q \in \mathbb{P}_\ell(E)$.

We note that there are multiple ways of defining the value and edge projections such that Assumption 2.5 is satisfied. An example choice based on a constrained least squares problem can be found in [26, 27], where the reader can find more details. We use the choice from [27] for the numerical experiments in section 4. Now, assuming we have a value and edge projection satisfying Assumption 2.5, we define the gradient projection and the local virtual element space $V_{h,\ell}^E$.

Definition 2.6. The *gradient projection* $\Pi_1^E : \tilde{V}_{h,\ell}^E \rightarrow [\mathbb{P}_{\ell-1}(E)]^2$ is defined as

$$\int_E \Pi_1^E v_h \cdot \mathbf{p} \, dx = - \int_E \Pi_0^E v_h \nabla \cdot \mathbf{p} \, dx + \sum_{e \subset \partial E} \int_e \Pi_0^e v_h \mathbf{p} \cdot \mathbf{n}_e \, ds \quad \forall \mathbf{p} \in [\mathbb{P}_{\ell-1}(E)]^2,$$

where \mathbf{n}_e denotes the unit outward normal vector to the edge e .

Definition 2.7. We define the *local virtual element space* $V_{h,\ell}^E$ as

$$V_{h,\ell}^E := \left\{ v_h \in \tilde{V}_{h,\ell}^E : (v_h - \Pi_0^E v_h, p)|_E = 0 \quad \forall p \in \mathbb{P}_\ell(E) \setminus \mathbb{P}_{\ell-2}(E) \right\},$$

for each element $E \in \mathcal{T}_h$.

The local space is characterised by the dof set Λ^E described by the dof tuple in (2.1), and proof that this dof set is unisolvant can be found in [20]. Importantly, as shown in [26], we have the following crucial property of our projection operators.

Lemma 2.8. *Assume that the value and edge projections satisfy Assumption 2.5. Then, for any $v_h \in V_{h,\ell}^E$, it holds that*

$$\Pi_0^E v_h = \mathcal{P}_\ell^E v_h \tag{2.2}$$

and

$$\Pi_1^E v_h = \mathcal{P}_{\ell-1}^E(\nabla v_h) \tag{2.3}$$

i.e., the value projection is the L^2 -orthogonal projection of order ℓ and the gradient projection is the L^2 -orthogonal projection of order $\ell - 1$ of the gradient.

2.3 Global spaces and the discrete forms

With the definition of the local spaces for each element $E \in \mathcal{T}_h$ in place, we can now define the global VEM space $V_{h,\ell}$ as

$$V_{h,\ell} := \left\{ v_h \in H_0^1(\Omega) : v_h|_E \in V_{h,\ell}^E \quad \forall E \in \mathcal{T}_h \right\} \subset H_0^1(\Omega),$$

where the global degrees of freedom are defined from the local degrees of freedom in the usual way, cf. [12], with local degrees of freedom corresponding to boundary vertices and boundary edges set to zero.

Lastly, we define the discrete forms required for the VEM formulation. We construct our virtual form elementwise as

$$a_h(z_h; v_h, w_h) = \sum_{E \in \mathcal{T}_h} a_h^E(z_h; v_h, w_h) \quad (2.4)$$

for any $z_h, v_h, w_h \in V_{h,\ell}$, where

$$a_h^E(z_h; v_h, w_h) := (\mu(\mathbf{x}, |\Pi_1^E z_h|) \Pi_1^E v_h, \Pi_1^E w_h)_E + S^E(z_h; (I - \Pi_0^E)v_h, (I - \Pi_0^E)w_h)$$

for some *admissible* stabilising form $S^E(\cdot, \cdot)$. We call the stabilisation $S^E(\cdot, \cdot)$ *admissible* if there exist positive constants C_*, C^* , independent of h, E , such that, for all $z_h, v_h \in V_{h,\ell}^E$ and all $E \in \mathcal{T}_h$,

$$C_* a^E(z_h; v_h, v_h) \leq S^E(z_h; v_h, v_h) \leq C^* a^E(z_h; v_h, v_h). \quad (2.5)$$

Definition 2.9 (Stabilisation). We define the stabilisation as

$$S^E(z_h; v_h, w_h) := M_\mu m_\mu \sum_{\lambda \in \Lambda^E} \lambda(v_h) \lambda(w_h),$$

making use of the standard *dofi-dofi* stabilisation; cf. [12].

Following the usual scaling argument from e.g. [12], it is clear that there exist positive constants β_*, β^* such that for any $z_h \in V_{h,\ell}$,

$$\beta_* \int_E \nabla v_h \cdot \nabla v_h \, d\mathbf{x} \leq S^E(z_h; v_h, v_h) \leq \beta^* \int_E \nabla v_h \cdot \nabla v_h \, d\mathbf{x}.$$

From Assumption 1.1(b) with any $t > 0$ and $s = 0$, we have that

$$m_\mu \leq \mu(\mathbf{x}, t) \leq M_\mu. \quad (2.6)$$

Therefore, taking $t = |\nabla z_h|$ in (2.6), it is clear to see that (2.5) holds with $C_* := \beta_*(M_\mu)^{-1}$ and $C^* := \beta^*(m_\mu)^{-1}$.

Remark 2.10. Alternatively, we could follow the stabilisation approach taken in [1, 18] and define the stabilisation as

$$S^E(z_h; v_h, w_h) := \mu_E(\mathbf{x}, |\Pi_1^{E,0} z_h|) \sum_{\lambda \in \Lambda^E} \lambda(v_h) \lambda(w_h),$$

where $\Pi_1^{E,0}$ denotes the gradient projection onto the space of constant polynomials, that is, $\Pi_1^{E,0} : \tilde{V}_{h,\ell}^E \rightarrow [\mathbb{P}_0(E)]^2$, and $\mu_E(\cdot)$ denotes the average of the function μ on the element

E . It is straightforward to show that this choice of stabilisation also satisfies (2.5). We note that this is the stabilisation we use in section 4; however both choices of stabilisation exhibit very similar numerical results. The only reason we use the linear stabilisation in Definition 2.9 throughout sections 2 and 3 is to ensure the validity of Lemma 2.12, without requiring further restrictions on the nonlinearity μ .

We also note the following important property holds. For any $v_h, z_h \in V_{h,\ell}$

$$\|\nabla v_h\|_{0,E} \leq C_4(S^E(z_h; v_h, v_h))^{1/2} \quad (2.7)$$

where $C_4 := \min((C_* M_\mu)^{-1/2}, (C_* m_\mu)^{-1/2})$. Additionally, for every $E \in \mathcal{T}_h$, we have the crucial stability property for any admissible stabilising form S^E : there exist constants α_*, α^* , independent of h and E , such that for all $v_h, z_h \in V_{h,\ell}^E$,

$$\alpha_* a^E(z_h; v_h, v_h) \leq a_h^E(z_h; v_h, v_h) \leq \alpha^* a^E(z_h; v_h, v_h). \quad (2.8)$$

2.4 The discrete problem

In this section we state the virtual element method for (1.1) and show, in Theorem 2.11, that it has a unique solution.

For order $\ell \geq 1$, the *virtual element method* discretisation of problem (1.4) reads as follows: find $u_h \in V_{h,\ell}$ such that

$$a_h(u_h; u_h, v_h) = L_h(v_h), \quad \forall v_h \in V_{h,\ell} \quad (2.9)$$

where the right hand side $L_h(v_h) = (f_h, v_h) := \sum_{E \in \mathcal{T}_h} (\Pi_0^E f, v_h)_E$, and the discrete form $a_h(\cdot; \cdot, \cdot)$ is defined in (2.4).

Theorem 2.11 (Existence and uniqueness of a discrete solution). *Under Assumption 1.1, for a given $f \in L^2(\Omega)$ there exists a unique element $u_h \in V_{h,\ell}$ such that (2.9) holds.*

The main tool required to prove Theorem 2.11, is the following Lemma which details two important properties of the discrete form a_h , the proof of which is a straightforward consequence of the stability properties (2.5), (2.8) as well as properties of the nonlinearity (1.2), (1.3).

Lemma 2.12. *The discrete form a_h defined in (2.4) admits the following properties.*

(a) a_h is Lipschitz continuous, in the sense that

$$|a_h(w_h; w_h, v_h) - a_h(z_h; z_h, v_h)| \leq C|w_h - z_h|_1|v_h|_1 \quad (2.10)$$

for all $w_h, z_h, v_h \in V_{h,\ell}$.

(b) a_h is strongly monotone in the sense that

$$a_h(w_h; w_h, w_h - z_h) - a_h(z_h; z_h, w_h - z_h) \geq C|w_h - z_h|_1^2 \quad (2.11)$$

for all $w_h, z_h \in V_{h,\ell}$.

We omit the proof of Theorem 2.11 since we can directly apply results from the theory of monotone operators as detailed in [36, Theorem 2.5] with [36, Lemma 2.2 and Lemma 2.3] replaced by Lemma 2.12.

3 A posteriori error analysis

In this section we carry out the a posteriori error analysis for the standard H^1 seminorm $|\cdot|_1$; we note that due to the boundary conditions as well as the Poincaré inequality, this is indeed a norm on $V_{h,\ell} \subset H_0^1(\Omega)$.

For the remainder of this paper, for ease of presentation we drop the dependence of μ on \mathbf{x} and simply write $\mu(t)$ in place of $\mu(\mathbf{x}, t)$.

3.1 Approximation properties

In order to carry out the a posteriori analysis, we require the following approximation result for the virtual element spaces defined in section 2. The proof of the following result for the original VEM space of [12] can be found in [39] for the two dimensional case, and has been extended to three dimensions in [19] for the virtual element spaces of [20] which are the same as those presented in this paper.

Theorem 3.1 (Approximation using VEM functions). *Under Assumption 2.1, for any $w \in H^1(\Omega)$, there exists $w_I \in V_{h,\ell}$ such that for all $E \in \mathcal{T}_h$,*

$$\|w - w_I\|_{0,E} + h_E|w - w_I|_{1,E} \leq C_5 h_E|w|_{1,E}, \quad (3.1)$$

where the constant C_5 depends only on ℓ and the mesh regularity.

3.2 The residual equation

We begin this section by deriving our *residual equation*. In order to do so, we define the *error* $\xi := u - u_h \in H_0^1(\Omega)$, where u is the weak solution to (1.4) and u_h is the virtual element solution to (2.9). For any $E \in \mathcal{T}_h$, using property assumption (1.3), we see that

$$C_2|u - u_h|_1^2 = C_2 \sum_{E \in \mathcal{T}_h} \int_E |\nabla(u - u_h)|^2 \, d\mathbf{x}$$

$$\begin{aligned}
&\leq \sum_{E \in \mathcal{T}_h} \int_E \mu(|\nabla u|) \nabla u \cdot \nabla (u - u_h) - \mu(|\nabla u_h|) \nabla u_h \cdot \nabla (u - u_h) \, d\mathbf{x} \\
&= \sum_{E \in \mathcal{T}_h} [a^E(u; u, \xi) - a^E(u_h; u_h, \xi)]. \tag{3.2}
\end{aligned}$$

Therefore, since u and u_h are the solutions to (1.4) and (2.9), respectively, for any $\chi \in V_{h,\ell}$ we have

$$\begin{aligned}
\sum_{E \in \mathcal{T}_h} [a^E(u; u, \xi) - a^E(u_h; u_h, \xi)] &= \sum_{E \in \mathcal{T}_h} [(f, \xi)_E - a^E(u_h; u_h, \chi) - a^E(u_h; u_h, \xi - \chi)] \\
&= \sum_{E \in \mathcal{T}_h} [(f, \xi)_E - (f_h, \chi)_E + a_h^E(u_h; u_h, \chi) - a^E(u_h; u_h, \chi) - a^E(u_h; u_h, \xi - \chi)] \\
&= \sum_{E \in \mathcal{T}_h} [(f, \xi - \chi)_E + (f - f_h, \chi)_E + a_h^E(u_h; u_h, \chi) \\
&\quad - a^E(u_h; u_h, \chi) - a^E(u_h; u_h, \xi - \chi)]. \tag{3.3}
\end{aligned}$$

3.3 Upper bounds (reliability)

To derive computable (reliable) upper bounds on the error, we estimate each term in the residual equation (3.3) in turn. Now, for any $w \in H_0^1(\Omega)$, we introduce the gradient projection $\Pi_1^E u_h$ of u_h and recall that $\Pi_1^E u_h = \mathcal{P}_{\ell-1}^E \nabla u_h$ (see (2.3) in Lemma 2.8); hence,

$$\begin{aligned}
a^E(u_h; u_h, w) &= \int_E \mu(|\nabla u_h|) \nabla u_h \cdot \nabla w \, d\mathbf{x} \\
&= \int_E (\mu(|\nabla u_h|) \nabla u_h \cdot \nabla w - \mu(|\Pi_1^E u_h|) \Pi_1^E u_h \cdot \nabla w) \, d\mathbf{x} \\
&\quad + \int_E \mu(|\Pi_1^E u_h|) \Pi_1^E u_h \cdot \nabla w \, d\mathbf{x}.
\end{aligned}$$

Using integration by parts on the term on the second line, we see that

$$\begin{aligned}
a^E(u_h; u_h, w) &= \int_E (\mu(|\nabla u_h|) \nabla u_h - \mu(|\mathcal{P}_{\ell-1}^E \nabla u_h|) \mathcal{P}_{\ell-1}^E \nabla u_h) \cdot \nabla w \, d\mathbf{x} \\
&\quad - \int_E \nabla \cdot (\mu(|\mathcal{P}_{\ell-1}^E \nabla u_h|) \mathcal{P}_{\ell-1}^E \nabla u_h) w \, d\mathbf{x} \\
&\quad + \sum_{e \subset \partial E} \int_e [\mu(|\mathcal{P}_{\ell-1}^E \nabla u_h|) \mathcal{P}_{\ell-1}^E \nabla u_h] w \, ds.
\end{aligned}$$

Furthermore, we introduce the polynomial approximation of order ℓ , $\mu_h(t) = \mathcal{P}_\ell^E(\mu(t))$, of the coefficient μ .

$$\begin{aligned}
a^E(u_h; u_h, w) &= \int_E (\mu(|\nabla u_h|) \nabla u_h - \mu(|\mathcal{P}_{\ell-1}^E \nabla u_h|) \mathcal{P}_{\ell-1}^E \nabla u_h) \cdot \nabla w \, d\mathbf{x} \\
&\quad + \int_E (\nabla \cdot (\mu_h(|\mathcal{P}_{\ell-1}^E \nabla u_h|) \mathcal{P}_{\ell-1}^E \nabla u_h) - \nabla \cdot (\mu(|\mathcal{P}_{\ell-1}^E \nabla u_h|) \mathcal{P}_{\ell-1}^E \nabla u_h)) w \, d\mathbf{x} \\
&\quad - \int_E \nabla \cdot (\mu_h(|\mathcal{P}_{\ell-1}^E \nabla u_h|) \mathcal{P}_{\ell-1}^E \nabla u_h) w \, d\mathbf{x} \\
&\quad + \sum_{e \subset \partial E} \left(\int_e (\llbracket \mu(|\mathcal{P}_{\ell-1}^E \nabla u_h|) - \mu_h(|\mathcal{P}_{\ell-1}^E \nabla u_h|) \rrbracket) \mathcal{P}_{\ell-1}^E \nabla u_h) w \, ds \right. \\
&\quad \left. + \int_e (\llbracket \mu_h(|\mathcal{P}_{\ell-1}^E \nabla u_h|) \mathcal{P}_{\ell-1}^E \nabla u_h \rrbracket) w \, ds \right).
\end{aligned}$$

Substituting this into (3.3) with $w = \xi - \chi$, we see that

$$\begin{aligned}
\sum_{E \in \mathcal{T}_h} a^E(u; u, \xi) - a^E(u_h; u_h, \xi) &= \sum_{E \in \mathcal{T}_h} \left((f - f_h, \chi)_E + a_h^E(u_h; u_h, \chi) - a^E(u_h; u_h, \chi) \right. \\
&\quad + (R^E, \xi - \chi)_E + (\theta^E, \xi - \chi)_E + (B^E, \nabla(\xi - \chi))_E \\
&\quad \left. - \sum_{e \subset \partial E} ((J^e, \xi - \chi)_{0,e} + (\theta^e, \xi - \chi)_{0,e}) \right) \tag{3.4}
\end{aligned}$$

where

$$\begin{aligned}
R^E &:= (f_h + \nabla \cdot \mu_h(|\mathcal{P}_{\ell-1}^E \nabla u_h|) \mathcal{P}_{\ell-1}^E \nabla u_h)|_E, \\
\theta^E &:= (f - f_h + \nabla \cdot (\mu(|\mathcal{P}_{\ell-1}^E \nabla u_h|) \mathcal{P}_{\ell-1}^E \nabla u_h - \mu_h(|\mathcal{P}_{\ell-1}^E \nabla u_h|) \mathcal{P}_{\ell-1}^E \nabla u_h))|_E, \\
B^E &:= (\mu(|\mathcal{P}_{\ell-1}^E \nabla u_h|) \mathcal{P}_{\ell-1}^E \nabla u_h - \mu(|\nabla u_h|) \nabla u_h)|_E, \\
J^e &:= \llbracket \mu_h(|\mathcal{P}_{\ell-1}^E \nabla u_h|) \mathcal{P}_{\ell-1}^E \nabla u_h \rrbracket|_e, \\
\theta^e &:= \llbracket (\mu(|\mathcal{P}_{\ell-1}^E \nabla u_h|) - \mu_h(|\mathcal{P}_{\ell-1}^E \nabla u_h|)) \mathcal{P}_{\ell-1}^E \nabla u_h \rrbracket|_e.
\end{aligned}$$

This leads us to the first crucial result of this subsection. This proof follows the ideas in [19].

Theorem 3.2 (Upper bound). *Let $u \in H_0^1(\Omega)$ be the weak solution given by (1.4) and $u_h \in V_{h,\ell}$ be its virtual element approximation obtained from (2.9). Then, the following error bound holds:*

$$|u - u_h|_1^2 \leq C \sum_{E \in \mathcal{T}_h} (\eta_E^2 + \Theta_E^2 + \mathcal{S}_E^2 + \Psi_E^2)$$

for some constant $C > 0$ which is independent of h , u , and u_h , where

$$\eta_E^2 := h_E^2 \|R^E\|_{0,E}^2 + \sum_{e \subset \partial E} h_e \|J^e\|_{0,e}^2,$$

$$\Theta_E^2 := h_E^2 \|\theta^E\|_{0,E}^2 + h_E^2 \|f - f_h\|_{0,E}^2 + \sum_{e \subset \partial E} h_e \|\theta^e\|_{0,e}^2,$$

$$\mathcal{S}_E^2 := S^E(u_h; (I - \mathcal{P}_\ell^E)u_h, (I - \mathcal{P}_\ell^E)u_h),$$

$$\Psi_E^2 := \|(\mathcal{P}_{\ell-1}^E - I)(\mu(|\mathcal{P}_{\ell-1}^E \nabla u_h|) \mathcal{P}_{\ell-1}^E \nabla u_h)\|_{0,E}^2.$$

Proof. Firstly, we take $\chi = \xi_I \in V_{h,\ell}$ in (3.4) to be the interpolation of $\xi = u - u_h$ into the VEM space $V_{h,\ell}$; then, it follows from (3.2) that

$$\begin{aligned} C_2 |\xi|_1^2 &\leq \sum_{E \in \mathcal{T}_h} a^E(u; u, \xi) - a^E(u_h; u_h, \xi) \\ &= \sum_{E \in \mathcal{T}_h} [(R^E, \xi - \xi_I)_E + (\theta^E, \xi - \xi_I)_E + (f - f_h, \xi_I)_E + (B^E, \nabla(\xi - \xi_I))_E \\ &\quad + (a_h^E(u_h; u_h, \xi_I) - a^E(u_h; u_h, \xi_I))] - \sum_{e \in \mathcal{E}_h} ((J^e, \xi - \xi_I)_{0,e} + (\theta^e, \xi - \xi_I)_{0,e}) \end{aligned}$$

Hence,

$$|\xi|_1^2 \leq C_2^{-1} \sum_{E \in \mathcal{T}_h} (T_1^E + T_2^E + T_3^E + T_4^E + T_5^E) - C_2^{-1} \sum_{e \in \mathcal{E}_h} (T_6^e + T_7^e).$$

We bound each term in turn, starting with T_1^E and T_2^E . We use the interpolation approximation properties of VEM functions (3.1) detailed in Theorem 3.1, and Cauchy-Schwarz, which gives us

$$T_1^E = (R^E, \xi - \xi_I)_E \leq \|R^E\|_{0,E} \|\xi - \xi_I\|_{0,E} \leq C_5 h_E \|R^E\|_{0,E} |\xi|_{1,E},$$

and

$$T_2^E = (\theta^E, \xi - \xi_I)_E \leq \|\theta^E\|_{0,E} \|\xi - \xi_I\|_{0,E} \leq C_5 h_E \|\theta^E\|_E |\xi|_{1,E}.$$

For T_3^E , we use properties of the value projection and the L^2 projection from Theorem 2.3. Since $f_h := \mathcal{P}_\ell^E f$, we observe that $(f - f_h, \mathcal{P}_\ell^E \xi_I) = 0$ and therefore

$$T_3^E = (f - f_h, \xi_I)_E = (f - f_h, \xi_I - \mathcal{P}_\ell^E \xi_I) \leq \|f - f_h\|_{0,E} C_3 h_E |\xi|_{1,E}.$$

Next, we look at bounding T_4^E . For this term we use the property of μ detailed in (1.2) as well as the interpolation results in (3.1). Therefore

$$\begin{aligned} T_4^E &= (B^E, \nabla(\xi - \xi_I))_E = (\mu(|\mathcal{P}_{\ell-1}^E \nabla u_h|) \mathcal{P}_{\ell-1}^E \nabla u_h - \mu(|\nabla u_h|) \nabla u_h, \nabla(\xi - \xi_I))_E \\ &\leq \int_E \left| \mu(|\mathcal{P}_{\ell-1}^E \nabla u_h|) \mathcal{P}_{\ell-1}^E \nabla u_h - \mu(|\nabla u_h|) \nabla u_h \cdot \nabla(\xi - \xi_I) \right| d\mathbf{x} \\ &\leq C_1 \|(\mathcal{P}_{\ell-1}^E - I) \nabla u_h\|_{0,E} |\xi - \xi_I|_{1,E} \\ &\leq C_1 C_5 \|(\mathcal{P}_{\ell-1}^E - I) \nabla u_h\|_{0,E} |\xi|_{1,E}. \end{aligned}$$

Since $\nabla \mathcal{P}_\ell^E u_h = \mathcal{P}_{\ell-1}^E \nabla \mathcal{P}_\ell^E u_h$, we use stability properties of the L^2 projection to see that

$$\begin{aligned} \|(\mathcal{P}_{\ell-1}^E - I) \nabla u_h\|_{0,E} &= \|(\mathcal{P}_{\ell-1}^E - I) \nabla u_h - (\mathcal{P}_{\ell-1}^E \nabla \mathcal{P}_\ell^E u_h - \nabla \mathcal{P}_\ell^E u_h)\|_{0,E} \\ &= \|(\mathcal{P}_{\ell-1}^E - I) \nabla(I - \mathcal{P}_\ell^E) u_h\|_{0,E} \leq C \|\nabla(I - \mathcal{P}_\ell^E) u_h\|_{0,E}. \end{aligned} \quad (3.5)$$

However, since ∇u_h is not a computable quantity, we need to bound this in terms of the stabilisation S^E . We apply (2.7) with $z_h = u_h$ and $v_h = (I - \mathcal{P}_\ell^E) u_h$ to see that

$$\|\nabla(I - \mathcal{P}_\ell^E) u_h\|_{0,E} \leq C_4 (S^E(u_h; (I - \mathcal{P}_\ell^E) u_h, (I - \mathcal{P}_\ell^E) u_h))^{1/2}. \quad (3.6)$$

Therefore,

$$T_4^E \leq C_1 C_4 C_5 |\xi|_{1,E} (S^E(u_h; (I - \mathcal{P}_\ell^E) u_h, (I - \mathcal{P}_\ell^E) u_h))^{1/2}.$$

Before we can estimate the edge terms, we turn our attention to T_5^E . We use property (1.2), together with properties of the L^2 projection to see that

$$\begin{aligned} T_5^E &:= a_h^E(u_h; u_h, \xi_I) - a^E(u_h; u_h, \xi_I) \\ &= \int_E \mu(|\mathcal{P}_{\ell-1}^E \nabla u_h|) \mathcal{P}_{\ell-1}^E \nabla u_h \cdot \mathcal{P}_{\ell-1}^E \nabla \xi_I - \mu(|\nabla u_h|) \nabla u_h \cdot \nabla \xi_I d\mathbf{x} \\ &\quad + S^E(u_h; (I - \Pi_0^E) u_h, (I - \Pi_0^E) \xi_I) \\ &= \int_E (\mu(|\mathcal{P}_{\ell-1}^E \nabla u_h|) \mathcal{P}_{\ell-1}^E \nabla u_h - \mu(|\nabla u_h|) \nabla u_h) \cdot \nabla \xi_I d\mathbf{x} \end{aligned}$$

$$\begin{aligned}
& + \int_E \mu(|\mathcal{P}_{\ell-1}^E \nabla u_h|) \mathcal{P}_{\ell-1}^E \nabla u_h \cdot (\mathcal{P}_{\ell-1}^E - I) \nabla \xi_I \, d\mathbf{x} + S^E(u_h; (I - \Pi_0^E)u_h, (I - \Pi_0^E)\xi_I) \\
& \leq (C_1 \|\mathcal{P}_{\ell-1}^E \nabla u_h - \nabla u_h\|_{0,E} + \|(\mathcal{P}_{\ell-1}^E - I)\mu(|\mathcal{P}_{\ell-1}^E \nabla u_h|) \mathcal{P}_{\ell-1}^E \nabla u_h\|_{0,E}) |\xi_I|_{1,E} \\
& \quad + S^E(u_h; (I - \Pi_0^E)u_h, (I - \Pi_0^E)\xi_I).
\end{aligned}$$

Using Cauchy-Schwarz, we see that

$$\begin{aligned}
S^E(u_h; (I - \Pi_0^E)u_h, (I - \Pi_0^E)\xi_I) & \leq (S^E(u_h; (I - \Pi_0^E)u_h, (I - \Pi_0^E)u_h))^{1/2} \\
& \quad \times (S^E(u_h; (I - \Pi_0^E)\xi_I, (I - \Pi_0^E)\xi_I))^{1/2}.
\end{aligned}$$

In order to bound the second part of this term, we use (2.6). Then,

$$\begin{aligned}
S^E(u_h; (I - \Pi_0^E)\xi_I, (I - \Pi_0^E)\xi_I) & \leq C^* \int_E \mu(|\nabla u_h|) \nabla(I - \Pi_0^E)\xi_I \cdot \nabla(I - \Pi_0^E)\xi_I \, d\mathbf{x} \\
& \leq C^* M_\mu \|\nabla(I - \Pi_0^E)\xi_I\|_{0,E}^2 \\
& \leq C^* M_\mu (C_3 |\xi_I|_{1,E})^2
\end{aligned}$$

where we have used Theorem 2.3 as well as the stability property detailed in (2.5) in the first line. Therefore,

$$S^E(u_h; (I - \Pi_0^E)u_h, (I - \Pi_0^E)\xi_I) \leq (C^* M_\mu)^{1/2} C_3 |\xi_I|_{1,E} (S^E(u_h; (I - \Pi_0^E)u_h, (I - \Pi_0^E)u_h))^{1/2}.$$

Recalling (3.6), we have

$$\begin{aligned}
T_5^E & \leq |\xi_I|_{1,E} (C_1 \|\mathcal{P}_{\ell-1}^E \nabla u_h - \nabla u_h\|_{0,E} + \|(\mathcal{P}_{\ell-1}^E - I)\mu(|\mathcal{P}_{\ell-1}^E \nabla u_h|) \mathcal{P}_{\ell-1}^E \nabla u_h\|_{0,E} \\
& \quad + (C^* M_\mu)^{1/2} C_3 (S^E(u_h; (I - \Pi_0^E)u_h, (I - \Pi_0^E)u_h))^{1/2}) \\
& \leq |\xi_I|_{1,E} (C_1 C_4 (S^E(u_h; (I - \mathcal{P}_\ell^E)u_h, (I - \mathcal{P}_\ell^E)u_h))^{1/2} \\
& \quad + \|(\mathcal{P}_{\ell-1}^E - I)\mu(|\mathcal{P}_{\ell-1}^E \nabla u_h|) \mathcal{P}_{\ell-1}^E \nabla u_h\|_{0,E} \\
& \quad + (C^* M_\mu)^{1/2} C_3 (S^E(u_h; (I - \mathcal{P}_\ell^E)u_h, (I - \mathcal{P}_\ell^E)u_h))^{1/2})
\end{aligned}$$

where we have used the L^2 property of the value projection (2.2) in the last step. Hence,

$$\begin{aligned}
T_5^E & \leq C |\xi_I|_{1,E} \left((S^E(u_h; (I - \mathcal{P}_\ell^E)u_h, (I - \mathcal{P}_\ell^E)u_h))^{1/2} \right. \\
& \quad \left. + \|(\mathcal{P}_{\ell-1}^E - I)\mu(|\mathcal{P}_{\ell-1}^E \nabla u_h|) \mathcal{P}_{\ell-1}^E \nabla u_h\|_{0,E} \right).
\end{aligned}$$

Lastly, we bound T_6^e and T_7^e . This requires the use of the standard scaled trace inequality which states that: for $v \in H^1(E)$

$$\|v\|_{0,e}^2 \leq C_6(h_E^{-1}\|v\|_{0,E}^2 + h_E\|\nabla v\|_{0,E}^2).$$

This, together with (3.1), gives us

$$T_6^e = \int_e J^e(\xi - \xi_I) \, ds \leq \|J^e\|_{0,e} \|\xi - \xi_I\|_{0,e} \leq C_6^{1/2} C_5 h_e^{1/2} \rho^{-1/2} |\xi|_{1,E^+ \cup E^-} \|J^e\|_{0,e}$$

and

$$T_7^e := \int_e \theta^e(\xi - \xi_I) \, ds \leq \|\theta^e\|_{0,e} \|\xi - \xi_I\|_{0,e} \leq C_6^{1/2} C_5 h_e^{1/2} \rho^{-1/2} |\xi|_{1,E^+ \cup E^-} \|\theta^e\|_{0,e}$$

where we have also applied part (b) of the mesh regularity Assumption 2.1.

The result now follows from Young's inequality since we have that

$$\begin{aligned} |u - u_h|_1 &\leq C \left\{ \left(\sum_{E \in \mathcal{T}_h} h_E^2 \|R^E\|_{0,E}^2 \right)^{1/2} + \left(\sum_{e \in \mathcal{E}_h} h_e \|J^e\|_{0,e}^2 \right)^{1/2} \right. \\ &\quad + \left(\sum_{E \in \mathcal{T}_h} h_E^2 \|\theta^E\|_{0,E}^2 \right)^{1/2} + \left(\sum_{E \in \mathcal{T}_h} h_E^2 \|f - f_h\|_{0,E}^2 \right)^{1/2} + \left(\sum_{e \in \mathcal{E}_h} h_e \|\theta^e\|_{0,e}^2 \right)^{1/2} \\ &\quad + \left(\sum_{E \in \mathcal{T}_h} S^E(u_h; (I - \mathcal{P}_\ell^E)u_h, (I - \mathcal{P}_\ell^E)u_h) \right)^{1/2} \\ &\quad \left. + \left(\sum_{E \in \mathcal{T}_h} \|(\mathcal{P}_{\ell-1}^E - I)\mu(|\mathcal{P}_{\ell-1}^E \nabla u_h|) \mathcal{P}_{\ell-1}^E \nabla u_h\|_{0,E}^2 \right)^{1/2} \right\}. \end{aligned}$$

□

Remark 3.3. We note that the estimator in Theorem 3.2 is also an estimator for the projected solution, as detailed in the next corollary.

Corollary 3.4. *Let $u \in H_0^1(\Omega)$ be the weak solution given by (1.4) and $u_h \in V_{h,\ell}$ be its virtual element approximation obtained from (2.9). Then, the following error bounds hold:*

$$|u - \Pi_0^h u_h|_1^2 \leq \overline{C} \sum_{E \in \mathcal{T}_h} (\eta_E^2 + \Theta_E^2 + \mathcal{S}_E^2 + \Psi_E^2) \quad (3.7)$$

$$\|\nabla u - \Pi_1^h u_h\|_0^2 \leq \widehat{C} \sum_{E \in \mathcal{T}_h} (\eta_E^2 + \Theta_E^2 + \mathcal{S}_E^2 + \Psi_E^2) \quad (3.8)$$

for constants $\overline{C}, \widehat{C} > 0$ which are independent of h , u , and u_h , where $\eta_E, \Theta_E, \mathcal{S}_E$, and Ψ_E are defined in Theorem 3.2.

Proof. First, we show (3.7) using (2.7) with $z_h = u_h$, and $v_h = u_h - \mathcal{P}_\ell^E u_h$. Together with L^2 projection properties of the value projection, we notice that

$$\begin{aligned} |u_h - \Pi_0^h u_h|_1^2 &= \sum_{E \in \mathcal{T}_h} \|\nabla(u_h - \mathcal{P}_\ell^E u_h)\|_{0,E}^2 \\ &\leq \sum_{E \in \mathcal{T}_h} C_4 S^E(u_h; u_h - \mathcal{P}_\ell^E u_h, u_h - \mathcal{P}_\ell^E u_h). \end{aligned}$$

Therefore, applying the triangle inequality, we see that

$$\begin{aligned} |u - \Pi_0^h u_h|_1^2 &\leq 2|u - u_h|_1^2 + 2|u_h - \Pi_0^h u_h|_1^2 \\ &\leq 2|u - u_h|_1^2 + 2 \sum_{E \in \mathcal{T}_h} C_4 S^E(u_h; u_h - \mathcal{P}_\ell^E u_h, u_h - \mathcal{P}_\ell^E u_h). \end{aligned}$$

The result now follows from Theorem 3.2.

To show (3.8), we note that

$$\|\nabla u_h - \Pi_1^h u_h\|_0^2 = \sum_{E \in \mathcal{T}_h} \|\nabla u_h - \Pi_1^E u_h\|_{0,E}^2 = \sum_{E \in \mathcal{T}_h} \|(I - \mathcal{P}_{\ell-1}^E) \nabla u_h\|_{0,E}^2$$

where we have applied Lemma 2.8. Therefore, applying (3.5) and (3.6) gives us the desired result as before. \square

3.4 Lower bounds (efficiency)

In this subsection we prove local lower bounds of the error in the H^1 -seminorm which demonstrates the efficiency of the error bound. In order to prove these lower bounds, we use standard properties of bubble functions introduced below.

A bubble function $\psi^E \in H_0^1(E)$ is constructed piecewise as the sum of the bubble functions [3] on each triangle of the mesh sub-triangulation [19]; cf. Remark 2.2.

Lemma 3.5 (Bubble functions). *For $E \in \mathcal{T}_h$, let ψ^E be the corresponding bubble function. Then, there exists a constant C_7 , independent of h_E such that for all $p \in \mathbb{P}_\ell(E)$*

$$C_7^{-1} \|p\|_{0,E}^2 \leq \int_E \psi^E p^2 \, dx \leq C_7 \|p\|_{0,E}^2,$$

and

$$C_7^{-1} \|p\|_{0,E} \leq \|\psi^E p\|_{0,E} + h_E |\psi^E p|_{1,E} \leq C_7 \|p\|_{0,E}.$$

Furthermore, for each $e \subset \partial E$, let ψ^e denote the corresponding edge bubble function. Then, for all $p \in \mathbb{P}_\ell(e)$,

$$C_7^{-1} \|p\|_{0,e}^2 \leq \int_e \psi^e p^2 \, ds \leq C_7 \|p\|_{0,e}^2,$$

and

$$h_E^{-1/2} \|\psi^e p\|_{0,E} + h_E^{1/2} |\psi^e p|_{1,E} \leq C_7 \|p\|_{0,e}$$

for a constant C_7 independent of h_E .

Theorem 3.6 (Local lower bound). *Let η_E, \mathcal{S}_E , and Θ_E be defined as in Theorem 3.2. Then, there exists a constant $C > 0$, independent of h, u , and u_h , such that for $E \in \mathcal{T}_h$*

$$\eta_E^2 \leq C \sum_{E' \in \omega_E} (\|\nabla(u - u_h)\|_{0,E'}^2 + \mathcal{S}_{E'}^2 + \Theta_{E'}^2)$$

where ω_E denotes the patch of elements containing E and its neighbouring elements; i.e.,

$$\omega_E := \{E' \in \mathcal{T}_h : \partial E' \cap \partial E \neq \emptyset\}.$$

Proof. Since $u \in H_0^1(\Omega)$ solves (1.4), it follows that

$$\sum_{E \in \mathcal{T}_h} a^E(u; u, \psi^E R^E) - a^E(u_h; u_h, \psi^E R^E) = \sum_{E \in \mathcal{T}_h} (f, \psi^E R^E)_E - a^E(u_h; u_h, \psi^E R^E).$$

We can now use the same approach that was used to derive (3.4) but with $w = \psi^E R^E$ to see that

$$\begin{aligned} a^E(u_h; u_h, \psi^E R^E) &= \int_E (\mu(|\nabla u_h|) \nabla u_h - \mu(|\mathcal{P}_{\ell-1}^E \nabla u_h|) \mathcal{P}_{\ell-1}^E \nabla u_h) \cdot \nabla(\psi^E R^E) \, d\mathbf{x} \\ &+ \int_E (\nabla \cdot (\mu_h(|\mathcal{P}_{\ell-1}^E \nabla u_h|) \mathcal{P}_{\ell-1}^E \nabla u_h) - \nabla \cdot (\mu(|\mathcal{P}_{\ell-1}^E \nabla u_h|) \mathcal{P}_{\ell-1}^E \nabla u_h)) \psi^E R^E \, d\mathbf{x} \\ &- \int_E \nabla \cdot (\mu_h(|\mathcal{P}_{\ell-1}^E \nabla u_h|) \mathcal{P}_{\ell-1}^E \nabla u_h) \psi^E R^E \, d\mathbf{x} \end{aligned}$$

where the boundary terms that appear in (3.4) are zero since $\psi^E|_{\partial E} = 0$. Therefore,

$$a^E(u; u, \psi^E R^E) - a^E(u_h; u_h, \psi^E R^E) = (R^E, \psi^E R^E)_E + (\theta^E, \psi^E R^E)_E + (B^E, \nabla(\psi^E R^E))_E.$$

We first observe using Assumption 1.1 that it also holds that

$$\begin{aligned} a^E(u; u, \psi^E R^E) - a^E(u_h; u_h, \psi^E R^E) &\leq \int_E \left| (\mu(|\nabla u|) \nabla u - \mu(|\nabla u_h|) \nabla u_h) \cdot \nabla (\psi^E R^E) \right| dx \\ &\leq C_1 \|\nabla(u - u_h)\|_{0,E} \|\nabla(\psi^E R^E)\|_{0,E}. \end{aligned}$$

Using the same argument as T_4^E in Theorem 3.2, we can show that

$$\begin{aligned} (B^E, \nabla(\psi^E R^E))_E &\leq C_1 \|(I - \mathcal{P}_{\ell-1}^E) \nabla u_h\|_{0,E} |\psi^E R^E|_{1,E} \\ &\leq C_1 C_4 (S^E(u_h; (I - \mathcal{P}_\ell^E) u_h, (I - \mathcal{P}_\ell^E) u_h))^{1/2} \|\nabla(\psi^E R^E)\|_{0,E}. \end{aligned}$$

Next, using Lemma 3.5 with $p = R^E \in \mathbb{P}_k(E)$ for some $k \in \mathbb{N}$, we have that

$$\begin{aligned} C_7^{-1} \|R^E\|_{0,E}^2 &\leq (R^E, \psi^E R^E)_E \\ &= a^E(u; u, \psi^E R^E) - a^E(u_h; u_h, \psi^E R^E) - (\theta^E, \psi^E R^E)_E - (B^E, \nabla(\psi^E R^E))_E \\ &\leq C_1 \|\nabla(u - u_h)\|_{0,E} \|\nabla(\psi^E R^E)\|_{0,E} + \|\theta^E\|_{0,E} \|\psi^E R^E\|_{0,E} \\ &\quad + C_1 C_4 (S^E(u_h; (I - \mathcal{P}_\ell^E) u_h, (I - \mathcal{P}_\ell^E) u_h))^{1/2} \|\nabla(\psi^E R^E)\|_{0,E} \\ &\leq \left(C_1 C_7 h_E^{-1} \|\nabla \xi\|_{0,E} + C_7 \|\theta^E\|_{0,E} \right. \\ &\quad \left. + C_1 C_4 C_7 h_E^{-1} (S^E(u_h; (I - \mathcal{P}_\ell^E) u_h, (I - \mathcal{P}_\ell^E) u_h))^{1/2} \right) \|R^E\|_{0,E} \end{aligned}$$

where we have used Lemma 3.5 again in the last line. Therefore

$$\tilde{C} h_E^2 \|R^E\|_{0,E}^2 \leq \|\nabla \xi\|_{0,E}^2 + h_E^2 \|\theta^E\|_{0,E}^2 + \mathcal{S}_E^2 \quad (3.9)$$

for some constant \tilde{C} .

For the edge residual part of η_E^2 , we extend J^e into ω_e through a constant prolongation in the normal direction to the edge e ; see e.g. [19]. This gives us $J^e \in \mathbb{P}_\ell(\omega_e) \subset V_{h,\ell}^{\omega_e} := V_{h,\ell}^{E^+} \cap V_{h,\ell}^{E^-}$ where $E^+ \cap E^- = e$. Then, using the derivation of (3.4) again with $w = \psi^e J^e$ and noting that the edge terms are no longer zero,

$$\begin{aligned} \sum_{E \in \mathcal{T}_h} a^E(u; u, \psi^e J^e) - a^E(u_h; u_h, \psi^e J^e) \\ = \sum_{E' \in \omega_e} (R^{E'}, \psi^e J^e)_{E'} + (\theta^{E'}, \psi^e J^e)_{E'} + (B^{E'}, \nabla(\psi^e J^e))_{E'} \end{aligned}$$

$$- (J^e, \psi^e J^e)_{0,e} - (\theta^e, \psi^e J^e)_{0,e}.$$

We use the same argument as before for the inner residual terms, as well as Lemma 3.5, to see that

$$\begin{aligned}
C_7^{-1} \|J^e\|_{0,e}^2 &\leq (J^e, \psi^e J^e)_{0,e} \\
&= \sum_{E' \in \omega_e} (R^{E'}, \psi^e J^e)_{E'} + (\theta^{E'}, \psi^e J^e)_{E'} + (B^{E'}, \nabla(\psi^e J^e))_{E'} \\
&\quad - (\theta^e, \psi^e J^e)_{0,e} + a(u_h; u_h, \psi^e J^e) - a(u; u, \psi^e J^e) \\
&\leq \sum_{E' \in \omega_e} \left((\|R^{E'}\|_{0,E'} + \|\theta^{E'}\|_{0,E'}) \|\psi^e J^e\|_{0,E'} \right. \\
&\quad \left. + (C_1 C_4 \mathcal{S}_{E'} + C_1 \|\nabla \xi\|_{0,E'}) \|\nabla(\psi^e J^e)\|_{0,E'} \right) + \|\theta^e\|_{0,e} \|\psi^e J^e\|_{0,e} \\
&\leq \sum_{E' \in \omega_e} \left(h_{E'}^{1/2} (\|R^{E'}\|_{0,E'} + \|\theta^{E'}\|_{0,E'}) \|J^e\|_{0,e} \right. \\
&\quad \left. + h_{E'}^{-1/2} (C_1 C_4 \mathcal{S}_{E'} + C_1 \|\nabla \xi\|_{0,E'}) \|J^e\|_{0,e} \right) + \|\theta^e\|_{0,e} \|J^e\|_{0,e}.
\end{aligned}$$

Firstly, we divide through by $\|J^e\|_{0,e}$ to see that

$$C_7^{-1} \|J^e\|_{0,e} \leq \|\theta^e\|_{0,e} + \sum_{E' \in \omega_e} h_{E'}^{1/2} (\|R^{E'}\|_{0,E'} + \|\theta^{E'}\|_{0,E'}) + h_{E'}^{-1/2} (C_1 C_4 \mathcal{S}_{E'} + C_1 \|\nabla \xi\|_{0,E'}).$$

Therefore, applying (3.9), we get the following

$$\begin{aligned}
\tilde{C} \|J^e\|_{0,e}^2 &\leq \|\theta^e\|_{0,e}^2 + \sum_{E' \in \omega_e} h_{E'} (\|R^{E'}\|_{0,E'}^2 + \|\theta^{E'}\|_{0,E'}^2) + h_{E'}^{-1} (\mathcal{S}_{E'}^2 + \|\nabla \xi\|_{0,E'}^2) \\
&\leq \|\theta^e\|_{0,e}^2 + \sum_{E' \in \omega_e} h_{E'} \|\theta^{E'}\|_{0,E'}^2 + 2h_{E'}^{-1} (\mathcal{S}_{E'}^2 + \|\nabla \xi\|_{0,E'}^2)
\end{aligned}$$

for some constant \tilde{C} . Hence, multiplying by h_e , and observing that $h_e \leq h_{E'}$, we see that

$$\begin{aligned}
\tilde{C} h_e \|J^e\|_{0,e}^2 &\leq h_e \|\theta^e\|_{0,e}^2 + \sum_{E' \in \omega_e} h_e h_{E'} \|\theta^{E'}\|_{0,E'}^2 + 2h_e h_{E'}^{-1} (\mathcal{S}_{E'}^2 + \|\nabla \xi\|_{0,E'}^2) \\
&= h_e \|\theta^e\|_{0,e}^2 + \sum_{E' \in \omega_e} h_{E'}^2 \|\theta^{E'}\|_{0,E'}^2 + 2(\mathcal{S}_{E'}^2 + \|\nabla \xi\|_{0,E'}^2)
\end{aligned}$$

Recalling the definition of η_E^2 and combining the estimates gives us the desired result. \square

Remark 3.7. We note that a direct consequence of Theorem 3.6 is a lower bound on the error between the solution u and the projected solution. That is,

$$\eta_E^2 \leq C \sum_{E' \in \omega_E} \left(|u - \Pi_0^{E'} u_h|_{1,E'}^2 + \mathcal{S}_{E'}^2 + \Theta_{E'}^2 \right) \quad (3.10)$$

and

$$\eta_E^2 \leq C \sum_{E' \in \omega_E} \left(\|\nabla u - \Pi_1^{E'} u_h\|_{0,E'}^2 + \mathcal{S}_{E'}^2 + \Theta_{E'}^2 \right) \quad (3.11)$$

with ω_E defined as in Theorem 3.6. Note that (3.10) and (3.11) follow directly from Theorem 3.6 combined with an application of the triangle inequality.

In the last part of this subsection, we prove the following lower bound for the inconsistency term Ψ_E^2 , where Ψ_E^2 is defined in Theorem 3.2.

Theorem 3.8 (Lower bound for inconsistency term). *There exists a constant $C > 0$ independent of h, u , and u_h such that*

$$\Psi_E^2 \leq C \left(\|\nabla(u - u_h)\|_{0,E}^2 + \mathcal{S}_E^2 + \|(\mathcal{P}_{\ell-1}^E - I)\mu(|\nabla u|)\nabla u\|_{0,E}^2 \right).$$

Proof. Recall the definition of Ψ_E^2 (Theorem 3.2), then note that we have

$$\begin{aligned} \Psi_E^2 &= \|(\mathcal{P}_{\ell-1}^E - I)(\mu(|\mathcal{P}_{\ell-1}^E \nabla u_h|)\mathcal{P}_{\ell-1}^E \nabla u_h)\|_{0,E}^2 \\ &= (\|\mathcal{P}_{\ell-1}^E(\mu(|\mathcal{P}_{\ell-1}^E \nabla u_h|)\mathcal{P}_{\ell-1}^E \nabla u_h) - \mathcal{P}_{\ell-1}^E(\mu(|\nabla u|)\nabla u)\|_{0,E} \\ &\quad + \|\mathcal{P}_{\ell-1}^E(\mu(|\nabla u|)\nabla u) - \mu(|\nabla u|)\nabla u\|_{0,E} \\ &\quad + \|\mu(|\nabla u|)\nabla u - \mu(|\mathcal{P}_{\ell-1}^E \nabla u_h|)\mathcal{P}_{\ell-1}^E \nabla u_h\|_{0,E})^2 \\ &\leq 2\|\mathcal{P}_{\ell-1}^E(\mu(|\mathcal{P}_{\ell-1}^E \nabla u_h|)\mathcal{P}_{\ell-1}^E \nabla u_h) - \mathcal{P}_{\ell-1}^E(\mu(|\nabla u|)\nabla u)\|_{0,E}^2 \\ &\quad + 2\|\mathcal{P}_{\ell-1}^E(\mu(|\nabla u|)\nabla u) - \mu(|\nabla u|)\nabla u\|_{0,E}^2 \\ &\quad + 2\|\mu(|\nabla u|)\nabla u - \mu(|\mathcal{P}_{\ell-1}^E \nabla u_h|)\mathcal{P}_{\ell-1}^E \nabla u_h\|_{0,E}^2 \\ &\leq 2\|(\mathcal{P}_{\ell-1}^E - I)\mu(|\nabla u|)\nabla u\|_{0,E}^2 + 4\|\mu(|\nabla u|)\nabla u - \mu(|\mathcal{P}_{\ell-1}^E \nabla u_h|)\mathcal{P}_{\ell-1}^E \nabla u_h\|_{0,E}^2 \end{aligned}$$

where we have used stability properties of the L^2 projection in the last step. We bound the last term by first applying (1.2) to see that

$$\|\mu(|\nabla u|)\nabla u - \mu(|\mathcal{P}_{\ell-1}^E \nabla u_h|)\mathcal{P}_{\ell-1}^E \nabla u_h\|_{0,E}^2 \leq C_1 \|\nabla u - \mathcal{P}_{\ell-1}^E \nabla u_h\|_{0,E}^2$$

$$\leq 2C_1(\|\nabla u - \nabla u_h\|_{0,E}^2 + \|\nabla u_h - \mathcal{P}_{\ell-1}^E \nabla u_h\|_{0,E}^2).$$

Using the same argument for term T_4^E in Theorem 3.2, see e.g. (3.6), we can show that

$$\|(I - \mathcal{P}_{\ell-1}^E) \nabla u_h\|_{0,E} \leq C_4(S^E(u_h; (I - \mathcal{P}_\ell^E)u_h, (I - \mathcal{P}_\ell^E)u_h))^{1/2}.$$

Therefore, the result follows. \square

4 Numerical results

In this section we present a collection of numerical results aimed at investigating the behaviour of the a posteriori error estimator derived in Theorem 3.2 and Corollary 3.4. Furthermore, we present an estimator driven adaptive algorithm and apply it to a selection of test problems.

The code used to carry out the simulations is based on the Distributed and Unified Numerics Environment (DUNE) software framework [11]. The virtual element method has been implemented within the DUNE-FEM module [29] and further implementation details can be found in [27]. DUNE is open source software implemented in C++; however, a user can readily carry out numerical experiments by describing mathematical models using the domain specific form language UFL [4] within the Python frontend [28, 30].

The aim of these experiments is to demonstrate that the second a posteriori error indicator (3.8) in Corollary 3.4 converges at the same rate as $\|\nabla u - \Pi_1^E u_h\|_{0,\Omega}$ on a sequence of adaptively refined meshes. We note that we consider this bound rather than Theorem 3.2 as ∇u_h is *not* a computable quantity. As is standard in residual-based a posteriori error estimation we set the constant \widehat{C} in Corollary 3.4 to 1 for simplicity; in general, this constant should be determined numerically, cf. [34]. We are then able to check whether the effectivity index,

$$\text{effectivity} := \frac{\left(\sum_{E \in \mathcal{T}_h} \eta_E^2 + \Theta_E^2 + \mathcal{S}_E^2 + \Psi_E^2\right)^{1/2}}{\|\nabla u - \Pi_1^E u_h\|_{0,\Omega}} \quad (4.1)$$

is roughly constant.

At each step of the adaptive algorithm we solve the virtual element formulation (2.9), compute the contribution of each element to the a posteriori error bound in Theorem 3.2, and refine the elements in \mathcal{T}_h with the largest contribution for the next iteration. In order to mark the elements with the largest error contribution, we employ a Dörfler marking strategy [32]; i.e., we construct the smallest subset of elements $\mathcal{T}_h^M \subset \mathcal{T}_h$ such that

$$\left(\sum_{E \in \mathcal{T}_h^M} \eta_E^2 + \Theta_E^2 + \mathcal{S}_E^2 + \Psi_E^2\right)^{1/2} \geq \theta \left(\sum_{E \in \mathcal{T}_h} \eta_E^2 + \Theta_E^2 + \mathcal{S}_E^2 + \Psi_E^2\right)^{1/2},$$

for a steering parameter $\theta \in (0, 1)$, by iteratively adding the element with the largest error contribution. For all our numerical experiments we use $\theta = 0.4$. In order to refine the elements we note that in our numerical experiments the elements are always convex and, hence, we can refine by connecting the midpoint of each planar edge to the element barycentre; cf. the mVEM package [42] for details on a MATLAB implementation. We note that for non-convex elements obeying Assumption 2.1 we can use a point to which the element is star-shaped instead. This refinement strategy introduces hanging nodes; however, these are handled automatically within the VEM framework. We note that there are other refinement strategies available, see e.g. [8, 16, 40].

4.1 Problem 1: smooth solution

In this first example we let $\Omega = (0, 1)^2$ and we define the nonlinear coefficient μ as follows

$$\mu(\mathbf{x}, |\nabla u|) = 2 + \frac{1}{1 + |\nabla u|^2}.$$

Furthermore, we take the right hand side f so that the exact solution is given by

$$u(x, y) = \sin(\pi x) \sin(\pi y).$$

We run the adaptive algorithm for the fixed order of approximation $\ell = 1, 2, 3$ on both a structured (4×4) quadrilateral grid and a smoothed Voronoi grid (of 16 elements); cf. Figure 2a and Figure 4a for the initial quadrilateral and Voronoi grids, respectively. In Figures 1a–1b and Figures 3a–3b, we compare the actual error of the gradient projection of the VEM solution and its a posteriori error bound from Corollary 3.4 to the number of degrees of freedom for the quadrilateral and Voronoi meshes, respectively, for the sequence of meshes generated by the adaptive mesh refinement algorithm. We observe that for both initial meshes the actual error and the error bound converges at a similar rate, with the error bound overestimating the true error by a roughly consistent factor; which is confirmed by Figures 1c and 3c which show that the effectivity index (4.1) for each mesh is roughly constant, although dependent on the approximation order. We remark that for virtual element methods the effectivity does appear slightly more oscillatory with a larger variance than usual; cf., for example, the effectivity indices for a discontinuous Galerkin finite element method [37].

Figures 2b–2c and 4b–4c display the mesh after 11 and 22 refinements for both the initial quadrilateral and Voronoi meshes, respectively, for $\ell = 1$. We note that the refinement is roughly uniform, with a slightly more concentrated refinement around the centre, as would be expected for the smooth analytical function considered.

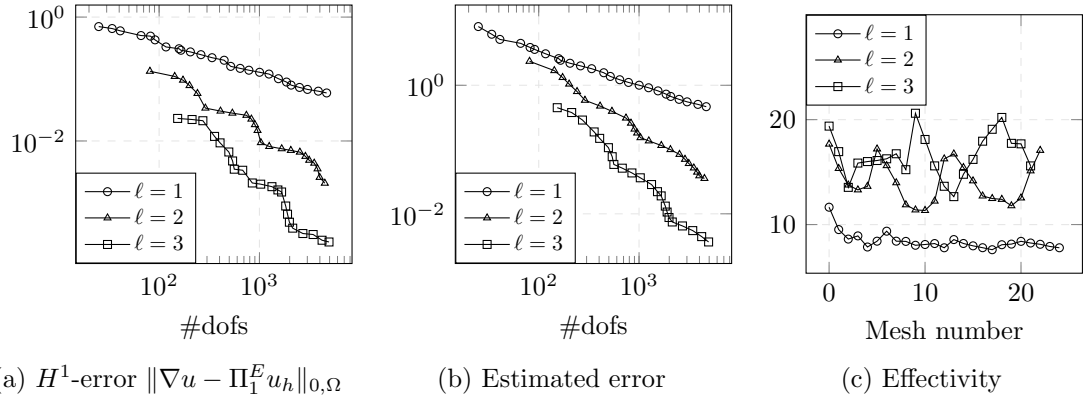


Figure 1: Problem 1: results from solving problem 1 (section 4.1) on the quadrilateral grid with adaptive refinement showing (a) convergence history in the $H^1(\Omega)$ seminorm, (b) estimated error, and (c) effectivity (4.1) of the estimator.

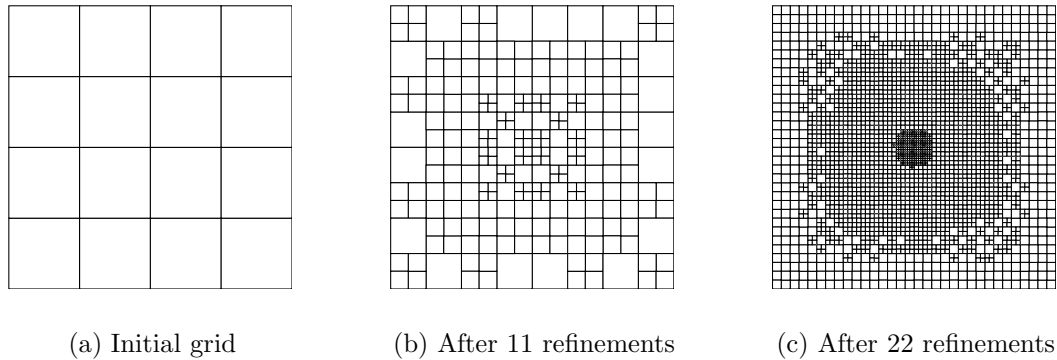


Figure 2: Problem 1: three mesh steps from the adaptive refinement of problem 1 (section 4.1) for the lowest order VEM ($\ell = 1$) with initial quadrilateral mesh.

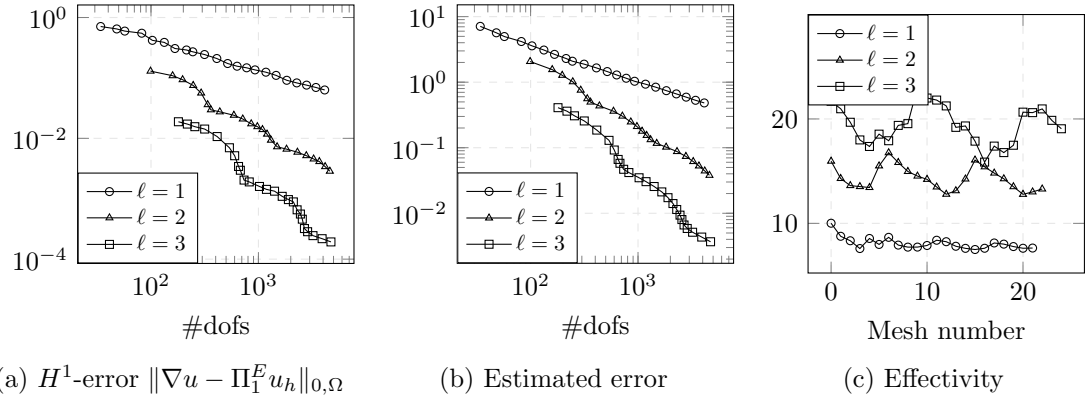


Figure 3: Problem 1: results from solving problem 1 (section 4.1) on the Voronoi grid with adaptive refinement showing (a) convergence history in the $H^1(\Omega)$ seminorm, (b) estimated error, and (c) effectivity (4.1) of the estimator.

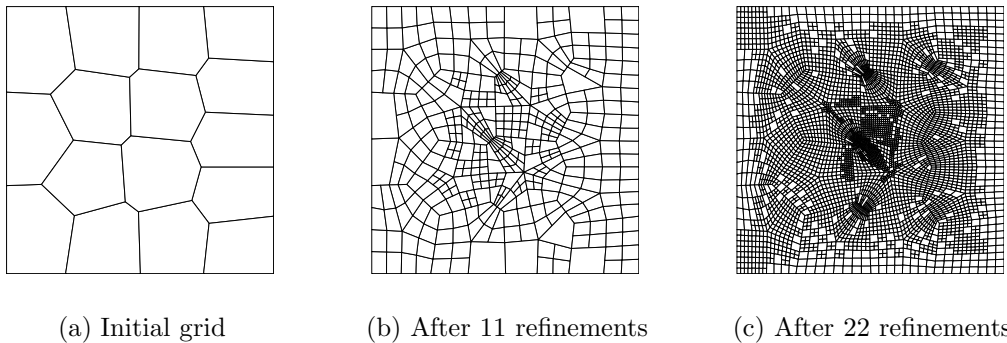


Figure 4: Problem 1: three mesh steps from the adaptive refinement of problem 1 (section 4.1) for the lowest order VEM ($\ell = 1$) with initial Voronoi mesh.

4.2 Problem 2: singular solution

In this example, which is also considered in e.g. [41], we take Ω to be the L-shaped domain $\Omega = (-1, 1)^2 \setminus [0, 1] \times (-1, 0]$ and choose the nonlinear coefficient to be

$$\mu(\mathbf{x}, |\nabla u|) = 1 + e^{-|\nabla u|^2}. \quad (4.2)$$

In this case, we choose the forcing f so that the exact solution to (1.1) is given by

$$u(r, \theta) = r^{2/3} \sin(2\theta/3)$$

where (r, θ) are the usual polar coordinates centred around $(0, 0)$. We note that here we additionally impose inhomogeneous Dirichlet boundary conditions. It is worth noting that in this example, u is analytic in $\bar{\Omega} \setminus \{\mathbf{0}\}$, but ∇u is singular at the origin.

We again run the adaptive algorithm for fixed order of approximation $\ell = 1, 2, 3$ on both a structured quadrilateral grid of 12 elements (Figure 6a) and a smoothed Voronoi grid of 21 elements (Figure 8a). Figures 5a–5b and Figures 7a–7b compare the actual error and its a posteriori error bound to the number of degrees of freedom for the quadrilateral and Voronoi meshes, respectively. Again, the actual error and the error bound appear to converge at a similar rate which is confirmed by the effectivity index in Figures 5c and 7c which appears roughly constant for all meshes.

For $\ell = 1$ an intermediate and final mesh from the adaptive algorithm are shown in Figures 6b–6c and 8b–8c for the quadrilateral and Voronoi meshes, respectively. As can be seen the refinement is focused around the singularity at the origin, as would be expected for this singular problem.

4.3 Problem 3: singular solution with a sharp Gaussian

For the final example, we again consider the L-shaped domain $\Omega = (-1, 1)^2 \setminus [0, 1] \times (-1, 0]$ from the previous problem, cf. 4.2, with the same nonlinearity (4.2), again with a singularity at the origin, but also with an additional sharp Gaussian. This is similar to the problem considered in [19] for a linear problem. Here, we set the forcing function f and inhomogeneous Dirichlet boundary conditions so that the exact solution is given by

$$u(x, y) = r^{2/3} \sin(2\theta/3) + e^{-(1000(x-0.5)^2 + 1000(y-0.5)^2)}.$$

with (r, θ) denoting the usual polar coordinates, and observe the sharp Gaussian at the point $(0.5, 0.5)$.

We run the adaptive algorithm for $\ell = 1, 2, 3$ on the same initial meshes as the previous problem; cf., Figures 10a and 12a. The comparison of the actual error and the error

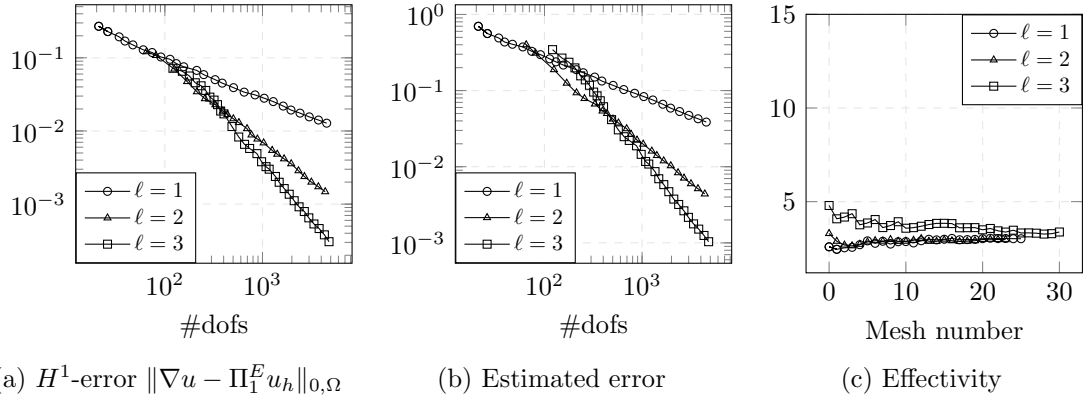


Figure 5: Problem 2: results from solving problem 2 (section 4.2) on the quadrilateral grid with adaptive refinement showing (a) convergence history in the $H^1(\Omega)$ seminorm, (b) estimated error, and (c) effectivity (4.1) of the estimator.

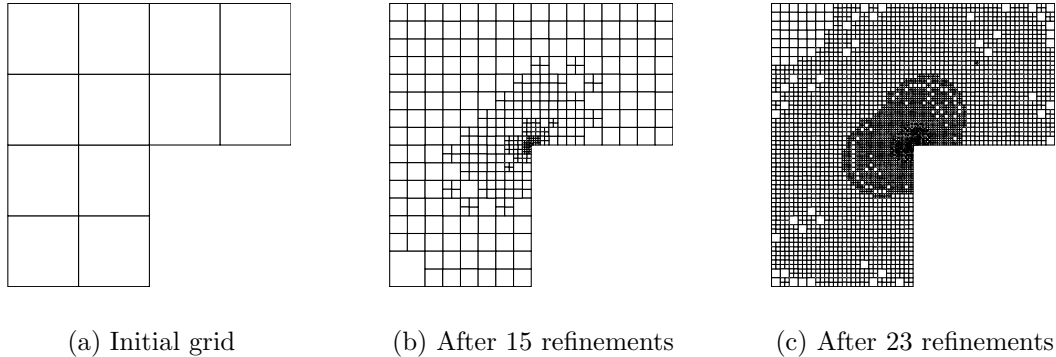


Figure 6: Problem 2: three mesh steps from the adaptive refinement of problem 2 (section 4.2) for the lowest order VEM ($\ell = 1$) with initial quadrilateral mesh.

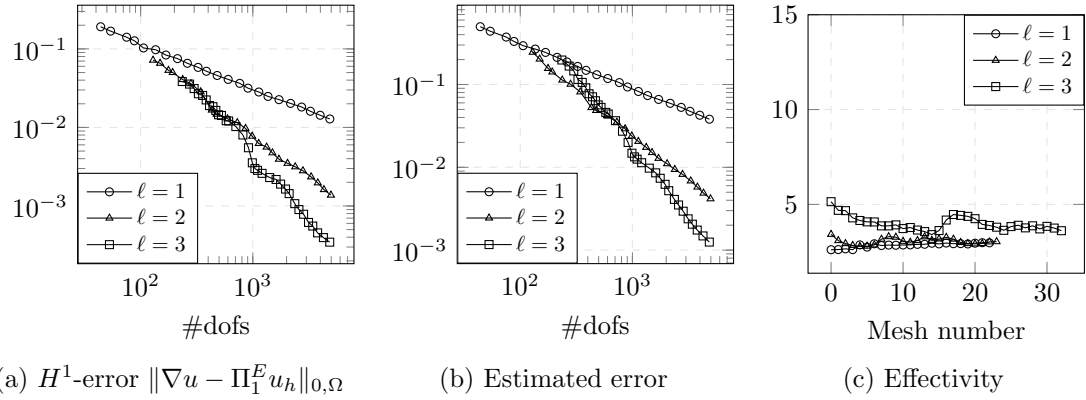


Figure 7: Problem 2: results from solving problem 2 (section 4.2) on the Voronoi grid with adaptive refinement showing (a) convergence history in the $H^1(\Omega)$ seminorm, (b) estimated error, and (c) effectivity (4.1) of the estimator.

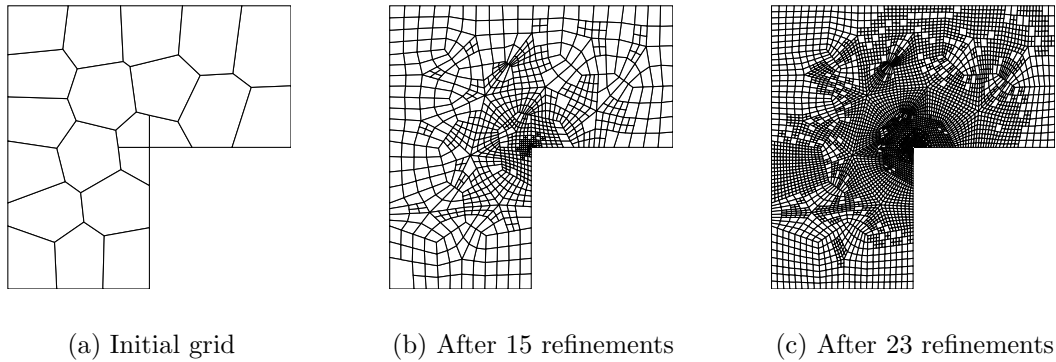


Figure 8: Problem 3: three mesh steps from the adaptive refinement of problem 2 (section 4.2) for the lowest order VEM ($\ell = 1$) with initial Voronoi mesh.

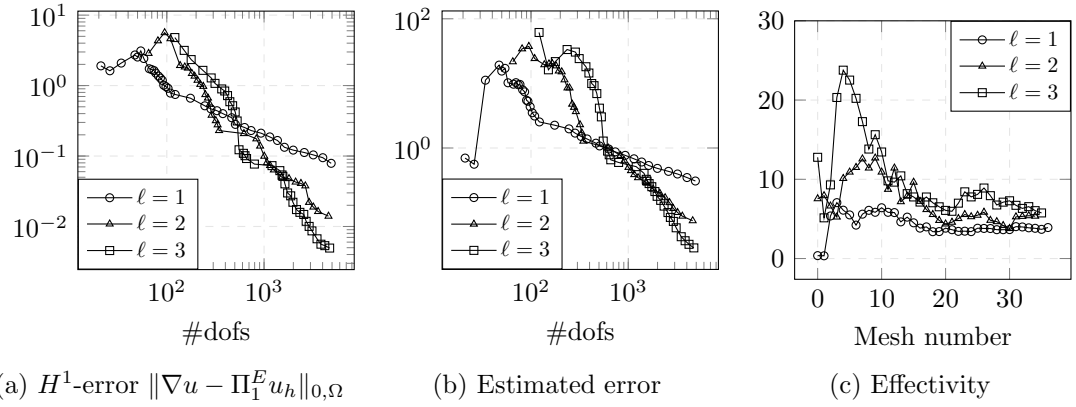


Figure 9: Problem 3: results from solving problem 1 (section 4.3) on the quadrilateral grid with adaptive refinement showing (a) convergence history in the $H^1(\Omega)$ seminorm, (b) estimated error, and (c) effectivity (4.1) of the estimator.

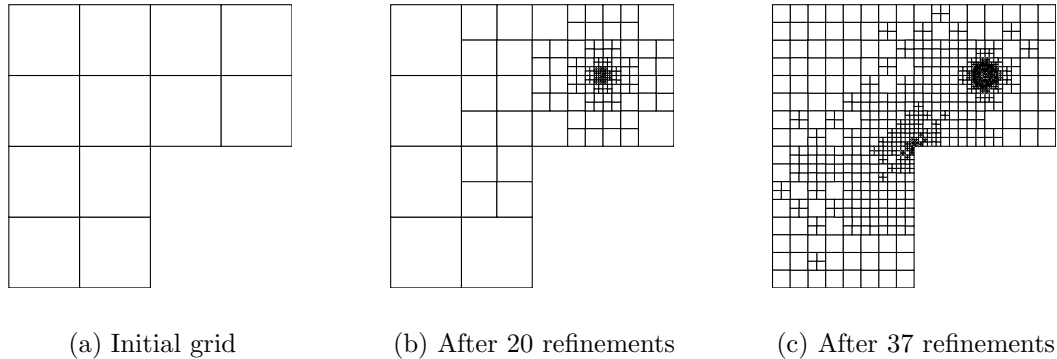


Figure 10: Problem 3: three mesh steps from the adaptive refinement of problem 3 (section 4.3) for the lowest order VEM ($\ell = 1$) with initial quadrilateral mesh.

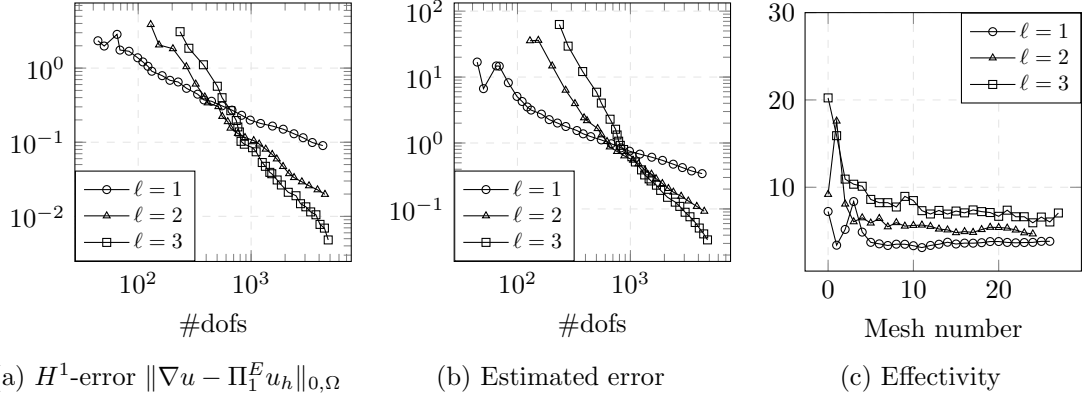


Figure 11: Problem 3: results from solving problem 1 (section 4.3) on the Voronoi grid with adaptive refinement showing (a) convergence history in the $H^1(\Omega)$ seminorm, (b) estimated error, and (c) effectivity (4.1) of the estimator.

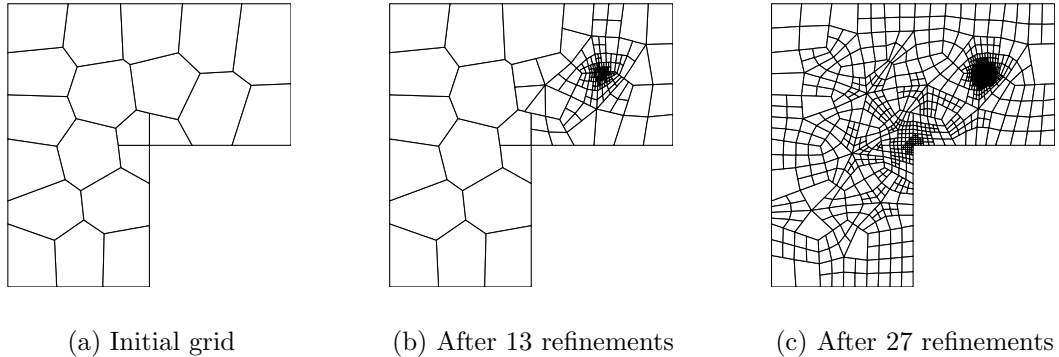


Figure 12: Problem 3: three mesh steps from the adaptive refinement of problem 3 (section 4.3) for the lowest order VEM ($\ell = 1$) with initial Voronoi mesh.

bound is shown in Figures 9a–9b and Figures 11a–11b. Here, we see that initial the error bound and true error behave slightly differently, but after some initial pre-asymptotic steps appear to start to converge at a similar rate. This is confirmed by the effectivity indices, cf. Figures 9c and 11c, which, are roughly constant after some initial steps. We note this initial behaviour likely occurs while the Gaussian is not sufficiently resolved.

An intermediate and final mesh for $\ell = 1$ are shown in Figures 10b–10c and 12b–12c. Here, it can be seen that the adaptive algorithm first refines around the sharp Gaussian at $(0.5, 0.5)$ until it is sufficiently resolved, and then further refinement is focused around this Gaussian and the singularity at the re-entrant corner.

5 Conclusion

In this paper we have developed a C^0 -conforming virtual element method of arbitrary approximation order for the discretisation of the second-order quasilinear elliptic PDE in two dimensions (1.1). We have applied the projection approach taken in [26, 27] and as a result we were able to define the discrete forms directly. In particular, we discretised the nonlinearity μ using the gradient projection Π_1^E which itself was shown to be the $L^2(E)$ -orthogonal projection of the gradient. Furthermore, we presented a posteriori error analysis and derived a fully computable residual based error estimator. Upper and lower bounds for the estimator were shown using techniques from [19] including a standard but important VEM interpolation result, which we detailed in Theorem 3.1. Finally, we presented a set of numerical results to study the behaviour of the proposed error estimator when using it to drive an adaptive algorithm. A variety of tests from the literature were carried out for two different sets of polygonal grids, and we demonstrated that the convergence rate of the a posteriori error bound and true error is roughly similar.

Funding

Both authors have been supported by Charles University Research programme no. PRIMUS/22/SCI/014.

References

[1] ADAK, D., ARRUTSELVI, M., NATARAJAN, E., AND NATARAJAN, S. On the implementation of virtual element method for nonlinear problems over polygonal

meshes. In *The Virtual Element Method and its Applications*. Springer, 2022, pp. 59–91.

- [2] AHMAD, B., ALSAEDI, A., BREZZI, F., MARINI, L. D., AND RUSSO, A. Equivalent projectors for virtual element methods. *Comput. Math. Appl.* 66, 3 (2013), 376–391.
- [3] AINSWORTH, M., AND ODEN, J. T. A posteriori error estimation in finite element analysis. *Comput. Methods Appl. Mech. Engrg.* 142, 1-2 (1997), 1–88.
- [4] ALNÆS, M. S., LOGG, A., ØLGAARD, K. B., ROGNES, M. E., AND WELLS, G. N. Unified form language: A domain-specific language for weak formulations of partial differential equations. *ACM Trans. Math. Softw.* 40, 2 (2014).
- [5] ANTONIETTI, P. F., BEIRÃO DA VEIGA, L., MANZINI, G., ET AL. *The virtual element method and its applications*. Springer, 2022.
- [6] ANTONIETTI, P. F., BEIRÃO DA VEIGA, L., SCACCHI, S., AND VERANI, M. A C^1 virtual element method for the Cahn–Hilliard equation with polygonal meshes. *SIAM J. Numer. Anal.* 54, 1 (2016), 34–56.
- [7] ANTONIETTI, P. F., BIGONI, N., AND VERANI, M. Mimetic finite difference approximation of quasilinear elliptic problems. *Calcolo* 52 (2015), 45–67.
- [8] ANTONIETTI, P. F., DASSI, F., AND MANUZZI, E. Machine learning based refinement strategies for polyhedral grids with applications to virtual element and polyhedral discontinuous galerkin methods. *J. Comput. Phys.* 469 (2022), 111531.
- [9] ANTONIETTI, P. F., MANZINI, G., SCACCHI, S., AND VERANI, M. A review on arbitrarily regular conforming virtual element methods for second- and higher-order elliptic partial differential equations. *Math. Models Methods Appl. Sci.* (2021).
- [10] ANTONIETTI, P. F., MANZINI, G., AND VERANI, M. The conforming virtual element method for polyharmonic problems. *Comput. Math. Appl.* 79, 7 (2020), 2021–2034.
- [11] BASTIAN, P., BLATT, M., DEDNER, A., ENGWER, C., KLÖFKORN, R., KORNHUBER, R., OHLBERGER, M., AND SANDER, O. A generic grid interface for parallel and adaptive scientific computing. part II: Implementation and tests in DUNE. *Computing* 82, 2–3 (2008), 121–138.
- [12] BEIRÃO DA VEIGA, L., BREZZI, F., CANGIANI, A., MANZINI, G., MARINI, L. D., AND RUSSO, A. Basic principles of virtual element methods. *Math. Models Methods Appl. Sci.* 23, 01 (2013), 199–214.
- [13] BEIRÃO DA VEIGA, L., LOVADINA, C., AND VACCA, G. Virtual elements for the Navier–Stokes problem on polygonal meshes. *SIAM J. Numer. Anal.* 56, 3 (2018), 1210–1242.

- [14] BEIRÃO DA VEIGA, L., AND MANZINI, G. Residual a posteriori error estimation for the virtual element method for elliptic problems. *ESAIM Math. Model. Numer. Anal.* 49, 2 (2015), 577–599.
- [15] BERRONE, S., AND BORIO, A. A residual a posteriori error estimate for the virtual element method. *Math. Models Methods Appl. Sci.* 27, 08 (2017), 1423–1458.
- [16] BERRONE, S., BORIO, A., AND D'AURIA, A. Refinement strategies for polygonal meshes applied to adaptive VEM discretization. *Finite Elem. Anal. Des.* 186 (2021), 103502.
- [17] BRENNER, S. C., AND SCOTT, L. R. *The mathematical theory of finite element methods*, 3rd ed. No. 15 in Texts in applied mathematics. Springer, New York, NY, 2008.
- [18] CANGIANI, A., CHATZIPANTELIDIS, P., DIWAN, G., AND GEORGULIS, E. H. Virtual element method for quasilinear elliptic problems. *IMA J. Numer. Anal.* 40, 4 (2020), 2450–2472.
- [19] CANGIANI, A., GEORGULIS, E. H., PRYER, T., AND SUTTON, O. J. A posteriori error estimates for the virtual element method. *Numer. Math.* 137 (2017), 857–893.
- [20] CANGIANI, A., MANZINI, G., AND SUTTON, O. J. Conforming and nonconforming virtual element methods for elliptic problems. *IMA J. Numer. Anal.* 37, 3 (2017), 1317–1354.
- [21] CHEN, C., HUANG, X., AND WEI, H. H^m -conforming virtual elements in arbitrary dimension. *SIAM J. Numer. Anal.* 60, 6 (2022), 3099–3123.
- [22] CHEN, F., YANG, M., AND ZHOU, Z. Two-grid virtual element discretization of quasilinear elliptic problem. *Math. Model. Anal.* 29, 1 (2024), 77–89.
- [23] CIARLET, P. G. *The finite element method for elliptic problems*. North-Holland Publishing Company, 1987.
- [24] CONGREVE, S., HOUSTON, P., SÜLI, E., AND WIHLER, T. P. Discontinuous Galerkin finite element approximation of quasilinear elliptic boundary value problems II: strongly monotone quasi-Newtonian flows. *IMA J. Numer. Anal.* 33, 4 (2013), 1386–1415.
- [25] DEDNER, A., AND HODSON, A. A higher order nonconforming virtual element method for the Cahn-Hilliard equation. *arXiv preprint arXiv:2111.11408* (2021).
- [26] DEDNER, A., AND HODSON, A. Robust nonconforming virtual element methods for general fourth-order problems with varying coefficients. *IMA J. Numer. Anal.* 42, 2 (2022), 1364–1399.
- [27] DEDNER, A., AND HODSON, A. A framework for implementing general virtual element spaces. *SIAM J. Sci. Comput.* 46, 3 (2024), B229–B253.

[28] DEDNER, A., KLOEFKORN, R., AND NOLTE, M. Python bindings for the DUNE-FEM module. *Zenodo 10* (2020).

[29] DEDNER, A., KLÖFKORN, R., NOLTE, M., AND OHLBERGER, M. A generic interface for parallel and adaptive discretization schemes: abstraction principles and the DUNE-FEM module. *Computing* 90, 3-4 (2010), 165–196.

[30] DEDNER, A., AND NOLTE, M. The Dune Python module. *Computer Science - Mathematical Software* (2018).

[31] DI PIETRO, D., AND DRONIQU, J. A Hybrid High-Order method for Leray–Lions elliptic equations on general meshes. *Math. Comp.* 86, 307 (2017), 2159–2191.

[32] DÖRFLER, W. A convergent adaptive algorithm for Poisson’s equation. *SIAM J. Numer. Anal.* 33, 3 (1996), 1106–1124.

[33] DOUGLAS JR, J., DUPONT, T., AND SERRIN, J. Uniqueness and comparison theorems for nonlinear elliptic equations in divergence form. *Arch. Ration. Mech. Anal.* 42, 3 (1971), 157–168.

[34] ERIKSSON, K., ESTEP, D. J., HANSBO, P., AND JOHNSON, C. Introduction to adaptive methods for differential equations. *Acta Numer.* 4 (1995), 105–158.

[35] GUDI, T., MALLIK, G., AND PRAMANICK, T. A hybrid high-order method for quasilinear elliptic problems of nonmonotone type. *SIAM J. Numer. Anal.* 60, 4 (2022), 2318–2344.

[36] HOUSTON, P., ROBSON, J., AND SÜLI, E. Discontinuous Galerkin finite element approximation of quasilinear elliptic boundary value problems I: The scalar case. *IMA J. Numer. Anal.* 25, 4 (2005), 726–749.

[37] HOUSTON, P., SÜLI, E., AND WIHLER, T. P. A posteriori error analysis of hp -version discontinuous Galerkin finite-element methods for second-order quasi-linear elliptic PDEs. *IMA J. Numer. Anal.* 28, 2 (2008), 245–273.

[38] LIU, W., AND BARRETT, J. W. Quasi-norm error bounds for the finite element approximation of some degenerate quasilinear elliptic equations and variational inequalities. *ESAIM Math. Model. Numer. Anal.* 28, 6 (1994), 725–744.

[39] MORA, D., RIVERA, G., AND RODRÍGUEZ, R. A virtual element method for the Steklov eigenvalue problem. *Math. Models Methods Appl. Sci.* 25, 08 (2015), 1421–1445.

[40] VAN HUYSSTEEN, D., RIVAROLA, F. L., ETSE, G., AND STEINMANN, P. On mesh refinement procedures for the virtual element method for two-dimensional elastic problems. *Comput. Methods Appl. Mech. Engrg.* 393 (2022), 114849.

[41] WIHLER, T., FRAUENFELDER, P., AND SCHWAB, C. Exponential convergence of the hp -DG-FEM for diffusion problems. *Comput. Math. Appl.* 46, 1 (2003), 183–205.

[42] YU, Y. Implementation of polygonal mesh refinement in matlab. *arXiv preprint arXiv:2101.03456* (2021).